# Accepted Manuscript

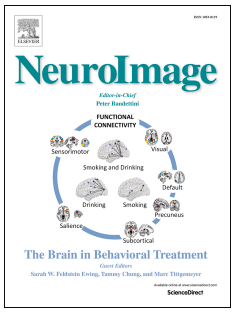


Intracranial high-γ connectivity distinguishes wakefulness from sleep

Ezequiel Mikulan, Eugenia Hesse, Lucas Sedeño, Tristán Bekinschtein, Mariano Sigman, María del Carmen García, Walter Silva, Carlos Ciraolo, Adolfo M. García, Agustín Ibáñez

PII: S1053-8119(17)31029-7

DOI: 10.1016/j.neuroimage.2017.12.015

Reference: YNIMG 14530

To appear in: *NeuroImage*

Received Date: 26 May 2017

Accepted Date: 6 December 2017

Please cite this article as: Mikulan, E., Hesse, E., Sedeño, L., Bekinschtein, Tristá., Sigman, M., García, Marí.del.Carmen., Silva, W., Ciraolo, C., García, A.M., Ibáñez, Agustí., Intracranial high-γ connectivity distinguishes wakefulness from sleep, *NeuroImage* (2018), doi: 10.1016/j.neuroimage.2017.12.015.

# Intracranial high-γ connectivity distinguishes wakefulness from sleep

Ezequiel Mikulan[1,2,3] *,#, Eugenia Hesse[1,2]*, Lucas Sedeño[1,2], Tristán Bekinschtein[3], Mariano Sigman[4], María del Carmen García[5], Walter Silva[5], Carlos Ciraolo[5], Adolfo M. García[1,2,6], Agustín Ibáñez[1,2,7,8,9],#

* Shared first authorship

[1] Laboratory of Experimental Psychology and Neuroscience (LPEN), Institute of Cognitive and Translational Neuroscience (INCYT), INECO Foundation, Favaloro University, Buenos Aires, Argentina

[2] National Scientific and Technical Research Council (CONICET), Buenos Aires, Argentina

[3] Consciousness and Cognition Lab, Department of Psychology, University of Cambridge , UK

[4] Di Tella University, Buenos Aires, Argentina

[5] Programa de Cirugía de Epilepsia, Hospital Italiano de Buenos Asires, Buenos Aires, Argentina.

[6] Faculty of Education, National University of Cuyo (UNCuyo), Mendoza, Argentina

[7] Universidad Autónoma del Caribe, Barranquilla, Colombia

[8] Center for Social and Cognitive Neuroscience (CSCN), School of Psychology, Universidad Adolfo Ibañez, Santiago de Chile, Chile

[9] Australian Research Council Centre of Excellence in Cognition and its Disorders, Sydney, Australia

Number of Pages: 34

Number of Figures: 9

Number of Tables: 1

Number of Words – Abstract: 193

Number of Words – Introduction: 634

Number of Words – Discussion: 1468

# Corresponding authors: Agustín Ibáñez (aibanez@ineco.org.ar) and Ezequiel Mikulan (e.mikulan@gmail.com)

Conflict of Interest

The authors declare no competing financial interests.

Acknowledgments

This work was supported by grants from CONICET, CONICYT/FONDECYT Regular (1170010), FONCyT-PICT [2012-0412 and 2012-1309], FONDAP 15150012 and INECO Foundation.

**Abstract**

*Neural synchrony in the γ-band is considered a fundamental process in cortical computation and communication and it has also been proposed as a crucial correlate of consciousness. However, the latter claim remains inconclusive, mainly due to methodological limitations, such as the spectral constraints of scalp-level electroencephalographic recordings or volume-conduction confounds. Here, we circumvented these caveats by comparing γ-band connectivity between two global states of consciousness via intracranial electroencephalography (iEEG), which provides the most reliable measurements of high-frequency activity in the human brain. Non-REM Sleep recordings were compared to passive-wakefulness recordings of the same duration in three subjects with surgically implanted electrodes. Signals were analyzed through the weighted Phase Lag Index connectivity measure and relevant graph theory metrics. We found that connectivity in the high-γ range (90-120 Hz), as well as relevant graph theory properties, were higher during wakefulness than during sleep and discriminated between conditions better than any other canonical frequency band. Our results constitute the first report of iEEG differences between wakefulness and sleep in the high-γ range at both local and distant sites, highlighting the utility of this technique in the search for the neural correlates of global states of consciousness.*



## Highlights

- IEEG recordings overcome the methodological limitations of other techniques
- IEEG high-γ connectivity is higher during wakefulness than during sleep
- It distinguishes between states better than any other canonical frequency band
- Connectivity differences are present at both local and distant sites

## 1. Introduction

Mainstream theories of consciousness converge on considering information integration across brain regions as a fundamental explanatory principle (Dehaene and Naccache, 2001; Tononi et al., 2016). However, no consensus exists on the putative mechanisms coordinating distributed neural activity. One possible candidate is neural synchrony (Uhlhaas et al., 2009). Indeed, temporal relationships between oscillatory processes are considered to be fundamental for both local and global coordinated brain activity

(Buzsáki, 2006). Moreover, phase relationships between activity in task-relevant areas prove critical for learning and memory, multisensory integration, selective attention, and working memory, among other domains (Wang, 2010). In particular, γ (30-90 Hz) and high-γ (> 90 Hz, or ε-band) synchronization seems critical for cortical computation (Buzsaki and Schomburg, 2015; Buzsaki and Wang, 2012; Fries, 2009), with temporal binding in the γ-range emerging as a potentially crucial marker of consciousness (Dehaene and Changeux, 2011; Engel and Singer, 2001).

However, the role of γ-synchronization in consciousness and cognition is not free of controversies. Studies typically compare healthy awake states with pathological or non-pathological loss of consciousness (e.g., coma and non-REM sleep, respectively; Bayne et al., 2016; Hohwy, 2009; Overgaard and Overgaard, 2010), or consciously vs. unconsciously perceived stimuli (Dehaene and Changeux, 2011). Propofol-induced (Murphy et al., 2011) and seizure-related (Pockett and Holmes, 2009) loss of consciousness have been shown to correlate with decreases, persistence, and increases of low-γ connectivity (Koch et al., 2016). Also, induced γ-band responses correlate with consciously perceived stimuli in multiple tasks, but extant results are confounded by several factors, such as artifacts from miniature saccades (Fries et al., 2008; Yuval-Greenberg et al., 2008).

Methodological limitations also pervade the field. The most common technique to study γ-band oscillations in humans is electroencephalography (EEG). EEG signals in the γ-range can be contaminated by external noise and muscular artifacts, leading many researchers to adopt an upper-limit of ~30 Hz in their analyses (Cohen, 2014). Magnetoencephalography features similar caveats (Muthukumaraswamy, 2013), and hemodynamic methods, such as functional magnetic resonance imaging, lack the temporal resolution to tap this frequency band (Huettel et al., 2014). To date, the only technique enabling reliable measurements of high-frequency activity in the human brain is intracranial EEG (iEEG; Lachaux et al., 2003; Muthukumaraswamy, 2013). In some

cases of pharmacoresistant epilepsies, surgical intervention planning requires monitoring brain activity via implanted electrodes (Engel et al., 2005; Engel, 2005) to locate epileptic foci for future resection. This provides inestimable information about brain functions, as electrodes record direct brain activity in both epileptic and non-epileptic sites, with the best spatial and temporal resolution available (Jacobs and Kahana, 2010).

Despite the proposed prominent role of γ-synchrony in consciousness, and even though γ-oscillations are present during both wakefulness and sleep (Le Van Quyen et al., 2010; Valderrama et al., 2012), only two iEEG studies have assessed synchronization of γ-oscillations above 40 Hz considering those two conditions. Bullock et al. (1995) found no differences between conditions, but they only computed connectivity among adjacent electrodes. Cantero et al. (2004) reported higher γ-coherence during wakefulness, but their analysis was restricted to the low-γ range (35-58 Hz). A major caveat in both cases is the use of the "coherence" measure, whose susceptibility to volume conduction and common reference problems calls for cautious interpretation of results (Bastos and Schoffelen, 2015). Moreover, until now, no human studies have investigated connectivity differences between wakefulness and sleep in frequency bands above 100 Hz.

Here, for the first time, we profit from iEEG to examine local and distributed high-γ connectivity during wakefulness and sleep. We assessed three patients with intracranial electrodes and compared phase synchronization between states via weighted Phase Lag Index (wPLI), a connectivity measure that circumvents volume conduction and common pick-up problems (Vinck et al., 2011). We found that connectivity in the high-γ band was higher during wakefulness and discriminated between states better than any other canonical frequency band.

## 2. Materials and Methods

*2.1 Subjects*. Three patients from an ongoing protocol (Canales-Johnson et al., 2015; Chennu et al., 2013; Hesse et al., 2016) with pharmacologically resistant epilepsy

participated in the study after signing informed consent. Subject 1 (S1) was a 19-year old right-handed female (13 years of education); Subject 2 (S2) was a 57-year-old left-handed male (16 years of education); Subject 3 (S3) was an 18-year-old right-handed male (12 years of education). Subjects were undergoing intracranial monitoring for which they had been implanted with depth electrodes (Engel, 2005) in loci entirely determined by clinical criteria (see Supplementary Tables ST1 to ST6 for further details). The study was conducted in accordance with the Declaration of Helsinki and approved by the local ethics committee.

*2.2 Data acquisition.* Direct recordings of local field potentials (LFPs) were obtained from semi-rigid, multi-lead electrodes (DIXI Medical Instruments), which contained 5 to 15 contact leads (0.8 mm diameter, 2 mm wide, 1.5 mm apart). Simultaneous iEEG and video were recorded using a standard video-iEEG monitoring system (Micromed S.p.A) with a 512 Hz sampling rate and common reference.

Whole-brain post-implant computerized tomography (CT; Emotion 16, Siemens) and structural magnetic resonance images (MRI; Eclipse 1.5T, Marconi Medical Systems Inc.) were obtained from each subject as part of their clinical procedure (El-Baz et al., 2011).

*2.3 Experimental Design.* Video-recordings and iEEG were visually inspected in search of night-sleep periods where subjects appeared behaviorally asleep (immobile, in recumbent position, with eyes closed; Goupil and Bekinschtein, 2012) and iEEG recordings were artifact-free. Fifteen to 25 minutes of recording were selected from each subject (S1: 20 m; S2: 15 m; S3: 25 m). For comparison purposes, recordings of the same duration were obtained from each subject while they were passively awake (S1: 20 m; S2: 15 m; S3: 25 m). As the clinical set-up precluded the possibility of scalp-EEG sleep-scoring, we confirmed the distinction between wakefulness and sleep using the Dimension of Activation (DA) measure (see below), which has been validated against other conventional scoring methods and has been successfully used in previous iEEG

research (Magnin et al., 2010). All recordings were performed in a quiet room and environmental conditions were held constant between conditions (same room and apparatus, lights turned off and no interferences).

*2.4 Data processing and Statistical Analysis*. Electrode location was determined by co-registering the patient's post-implant CT and MRI scans (Tao et al., 2009), on the 3D Slicer software (Fedorov et al., 2012). Further analyses were restricted to contacts that were located in non-dysplastic grey matter (Kabat and Krol, 2012) and proved free of clear epileptic activity (as identified by a neurologist specialized in epilepsy: MCG), namely, 51/68, 40/65, and 77/127 from S1, S2, and S3, respectively. To further assess the presence of artifacts and epileptic activity, we ensured that signal values did not exceed five times the channel mean and no consecutive samples exceeded five SDs from the gradient mean (Chen et al., 2013; Fell et al., 2008). Plots of electrode locations were created using the BrainNet Viewer toolbox (Xia et al., 2013).

Data was low-pass filtered at 240 Hz and notch filtered at 50, 100, 150, and 200 Hz using EEGLAB (Delorme and Makeig, 2004) on Matlab (Mathworks Inc.). The ensuing signals were then segmented into 16-second epochs (Magnin et al., 2010), with an automatic epoch rejection threshold of 150 μV peak-to-peak amplitude. To validate our distinction between wake and sleep recordings, the DA was calculated for each channel and epoch using a bipolar reference scheme and a temporal separation between samples of ~16 ms, following standard parameters (Magnin et al., 2010). The DA is a non-linear measure, based on the dimensional complexity approach (Achermann et al., 1994; Shen et al., 2003), which provides an index that can be used for identifying non-REM sleep periods (and sleep onset) from EEG and iEEG data (Rey et al., 2007). This measure is widely used in sleep research and has also been validated against conventional spectral measures (Acharya et al., 2005; Fell et al., 1996; Pereda et al., 1999). We employed it to validate our distinction between sleep and wake data by taking the average across channels, low-pass filtering it (Savitzky-Golay filter, window length = 15,

polynomial order = 3), and using a cut-off score of 5 (see Magnin et al., 2010). We also tested their difference by comparing their distributions using non-parametric permutation Welch *t*-tests (Cohen, 2014; Maris and Oostenveld, 2007) with $10^4$ permutations, and estimated *p*-values ($p_n$) based on the proportion of suprathreshold tests as:

$$p_n = \frac{B+1}{M+1} \tag{1}$$

where B corresponds to the number of random permutations in which a statistic greater or equal than the observed is obtained, and M represents the total number of random permutations sampled. We employed this approach for estimating p-values as it provides appropriate control of type-I and family-wise error rates (Phipson and Smyth, 2010).

Subsequent iEEG analyses were performed using the MNE toolbox (Gramfort et al., 2013; Gramfort et al., 2014) and custom scripts in Python. Data was segmented into 8-second epochs (to allow for at least 7 cycles of the lowest estimated frequency, see below) and re-referenced to the average of all grey-matter contacts. Weighted Phase Lag Index (wPLI) was calculated for each pair of electrodes on each condition (Vinck et al., 2011) for the three frequency bands of interest: low-γ (30-60 Hz), medium-γ (60-90 Hz), and high-γ (90-120 Hz). Spectral densities were estimated using the multitaper method provided by the MNE toolbox. The wPLI is a bivariate, phase-based functional connectivity measure that is computed as follows (Vinck et al., 2011):

$$wPLI = \frac{\left|E\{\left|I\{\mathrm{X}\}\right|\mathrm{sgn}(I\{X\})\}\right|}{E\{\left|I\{X\}\right|\}} \tag{2}$$

where E{.} is the expected value operator, *I{X}* denotes the imaginary part of the cross-spectrum between channels, and *sgn* the sign function.

WPLI was chosen as the connectivity measure because it has several advantages over other indexes. It measures the consistency in the phase difference between

channels, weighting the estimate by how far the difference is from 0º or 180º in the polar plane (see Vinck et al., 2011). Therefore, it is robust against volume conduction, which is instantaneous within iEEG measurement capabilities (0º or 180º; Cohen, 2014). Moreover, it affords a clear neurophysiological interpretation, unlike other types of measures as those derived from information theory (Cohen, 2014). Also, it proves robust against uncorrelated noise and inter-subject variation in sample size (Vinck et al., 2011). In addition, previous scalp EEG studies have successfully relied on it to distinguish between control subjects, patients in minimally conscious state and patients in vegetative state (Chennu et al., 2014), and between responsive and unresponsive subjects during propofol-induced transitions of consciousness (Chennu et al., 2016).

As γ-oscillations typically arise locally (Buzsaki and Wang, 2012) and co-detection probability of γ-oscillations decays with increasing distance during slow wave sleep (Valderrama et al., 2012), we computed the Pearson correlation coefficient of wPLI values and the Euclidean distance between contacts for each frequency band to verify that our results were not driven by local interactions. If connectivity values decreased with increasing distance (negative correlation), they could be assumed to depend on the distance between contacts.

We compared the connectivity results between states using two complementary strategies: from a network perspective and from an electrode perspective. In the former, we characterized the networks calculating each channel's Degree, a graph-theory metric which corresponds to the number of connections of the channel after binarizing the connectivity matrix by a certain threshold (Rubinov and Sporns, 2010). This approach reduces the dimensionality of the data and provides a quantification of relevant network properties. In particular, the Degree distribution is a measure of the density of the connections in the network (Rubinov and Sporns, 2010). It was chosen because it is the most fundamental network measure, it has been widely used for comparing brain networks (Bullmore and Sporns, 2009), and it directly quantifies the property

concerning our hypothesis of a difference in connection density between wakefulness and sleep. The graph-theory analysis was performed using the NetworkX toolbox (Hagberg et al., 2008). As subjects had different numbers of electrodes, Degrees were normalized by the subject's total number nodes. We compared the network's degree distribution at 100 ascending thresholds (0 to 1 in 0.01 steps) using non-parametric permutation Welch *t*-tests with $10^3$ permutations and correcting for multiple comparisons using pixel-based statistics (Cohen, 2014). Within this first strategy, we only performed between-conditions within-subject analyses because subjects had different electrode placement and it is not possible to compare networks that use different parcellation schemes (Honey et al., 2009; Wang et al., 2009). The non-parametric permutation approach was preferred over parametric tests because it is the recommended framework for comparing graph-theory-based measures, as it does not rely on specific data distributions (Cohen, 2014).

In order to test the specificity of the effect, we repeated the aforementioned procedure with other frequency bands: δ (1-4 Hz), θ (4-7 Hz), low-α (7-10 Hz), high-α (10-13 Hz), and β (13-30 Hz). The α band was subdivided to control for the effect of sleep spindles, whose frequency band approximately corresponds to high-α (De Gennaro and Ferrara, 2003). We also tested whether connectivity differences were associated with differences in power by running comparisons between conditions using the multitaper method, non-parametrical permutation Welch *t*-tests with $10^4$ permutations, *p*-values ($p_n$) based on the proportion of suprathreshold tests as described by Equation 1, and Holm-Bonferroni multiple comparisons correction (Cohen, 2014; Holm, 1979; Maris and Oostenveld, 2007; Phipson and Smyth, 2010).

The second analysis strategy had three objectives: to test the difference between conditions at the group level, to compare the discrimination performance of the studied frequency bands, and to account for possible subtle differences in epileptic activity between wakefulness and sleep. Interictal epileptiform discharges have been shown to

vary between wakefulness and sleep (Clemens et al., 2003; Sammaritano et al., 1991) and epileptic activity has been show to be related to neuronal networks dynamics (Pittau et al., 2014; Stefan and Lopes da Silva, 2013). Consequently, even though contacts with clear epileptiform activity were discarded from the analysis, it was still possible that our results were driven by subtle differences in epileptic activity between conditions. We therefore used an automatic detection algorithm, the Short Line Length detector (Gardner et al., 2007), from the RIPPLELAB toolbox (Navarrete et al., 2016), to find and classify interictal spikes and ripples (Jacobs et al., 2012). Then, we conducted a Generalized Estimating Equations (GEE) analysis for each frequency band, which included Condition (wake/sleep) as dependent variable; channel mean-wPLI, channel spikes, and channel ripples as predictors; and subjects as independent clusters. Robust estimation and independent working correlation structure were used in these analyses. Spikes and ripples were normalized by the total length of the recording to account for the difference in recording durations between subjects. The GEE method was chosen because of the dependent nature of within-subject observations (Aarts et al., 2014; Sainani, 2010). Collinearity was assessed via Variance Inflation Factor (VIF) with a threshold of 3 (O'brien, 2007) and goodness-of-fit of the models via quasi-likelihood under the independence model criterion (QIC), which is an extension of the Akaike's Information Criterion (AIC) for GEEs (Pan, 2001). The mean-wPLI of individual contacts were plotted in the MNI152 common space (Mazziotta et al., 1995), using the Nilearn toolbox (Abraham et al., 2014). Finally, we performed *post hoc* tests between conditions at each anatomical region, to further assess the topographical profile of the differences. To this end, we employed GEEs with target-regions as clusters, robust estimation and independent working correlation structure. The GEE method was again chosen because of the dependent nature of within-subject observations (Aarts et al., 2014). Results were corrected for multiple comparisons using the Holm-Bonferroni method (Holm, 1979). Mapping of coordinates to anatomical regions was performed

automatically using the *label4MRI* R package, following the Automated Anatomical Labeling naming-convention (Tzourio-Mazoyer et al., 2002).

All statistical analyses were performed on R software (R Core Team, 2015) and Python.

## 3. Results

The behavioral distinction of wakefulness and sleep recordings was validated by DA results (Figure 1). Wake data was consistently above the cut-off score of 5 and sleep data was consistently below it for the 3 subjects (Magnin et al., 2010). Their difference was significant in all cases (S1: t(154.33) = 26.03, $p_n < .001$; S2: t(84.48) = 73.86, $p_n < .001$; S3: t(180.22) = 61.66, $p_n < .001$).

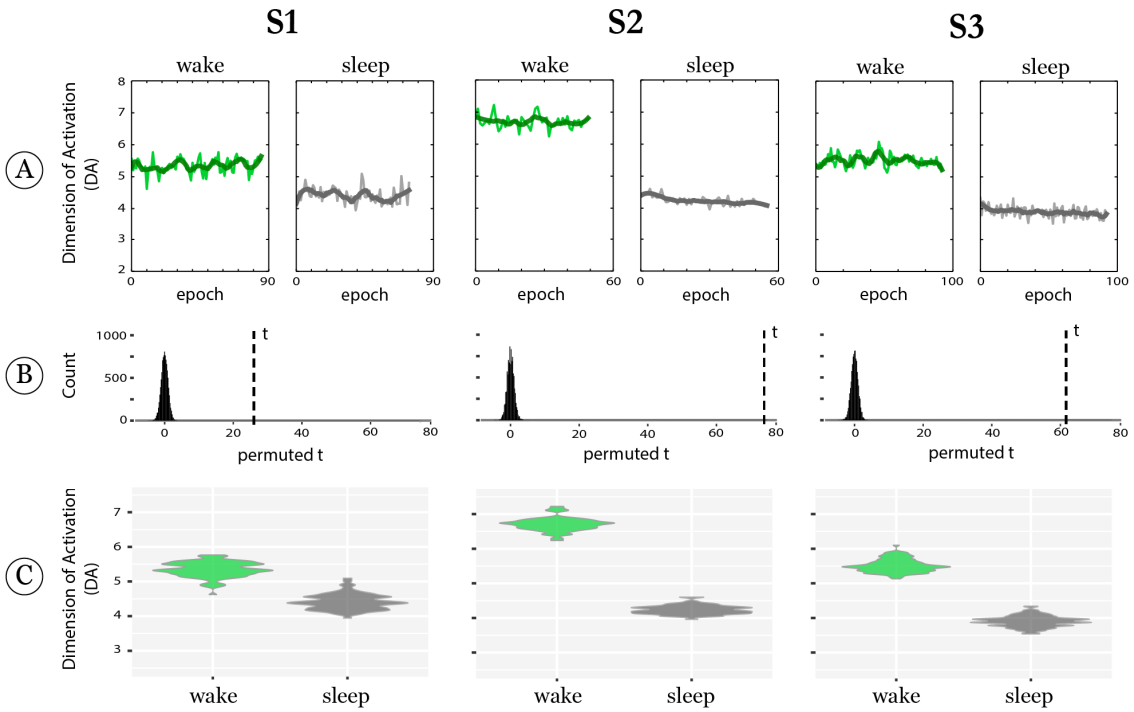


**Figure 1. Validation of the behavioral distinction between wakefulness and sleep data**. A) Low-pass filtered (dark lines) Dimension of Activation (DA) scores averaged across channels (light lines) were consistently above the cut-off score of 5 on wake condition and consistently below it on sleep condition. B) Histogram of the non-parametric permutation test t-values and t-value of the original comparison (dotted vertical line). No permuted comparison yielded a statistic above the one obtained in the original comparison. C) Distribution of DA values for each condition.

Visual inspection of wPLI distributions (Figure 2A) and matrix representations (Figure 2B) suggests that the wake condition had higher connectivity in the three frequency bands of interest for the three subjects, except for the medium- and low-γ bands in S2 (see also Supplementary Figure SF1 for other frequency bands). Interestingly, high connectivity values in the high-γ range seem to be distributed across all intra- and inter-lobular electrode pairs with the exception of temporo-temporal and parieto-parietal pairs in S1. In addition, relatively high values do not appear to be circumscribed to neighboring pairs, as would be shown by clustering of high values along the matrices' top-left to bottom-right diagonal. Remarkably, some pairs showed relatively high values during the sleep condition, but these were restricted to adjacent or within-lobe contacts (e.g. temporal lobe sites in S1 and occipital lobe sites in S3).

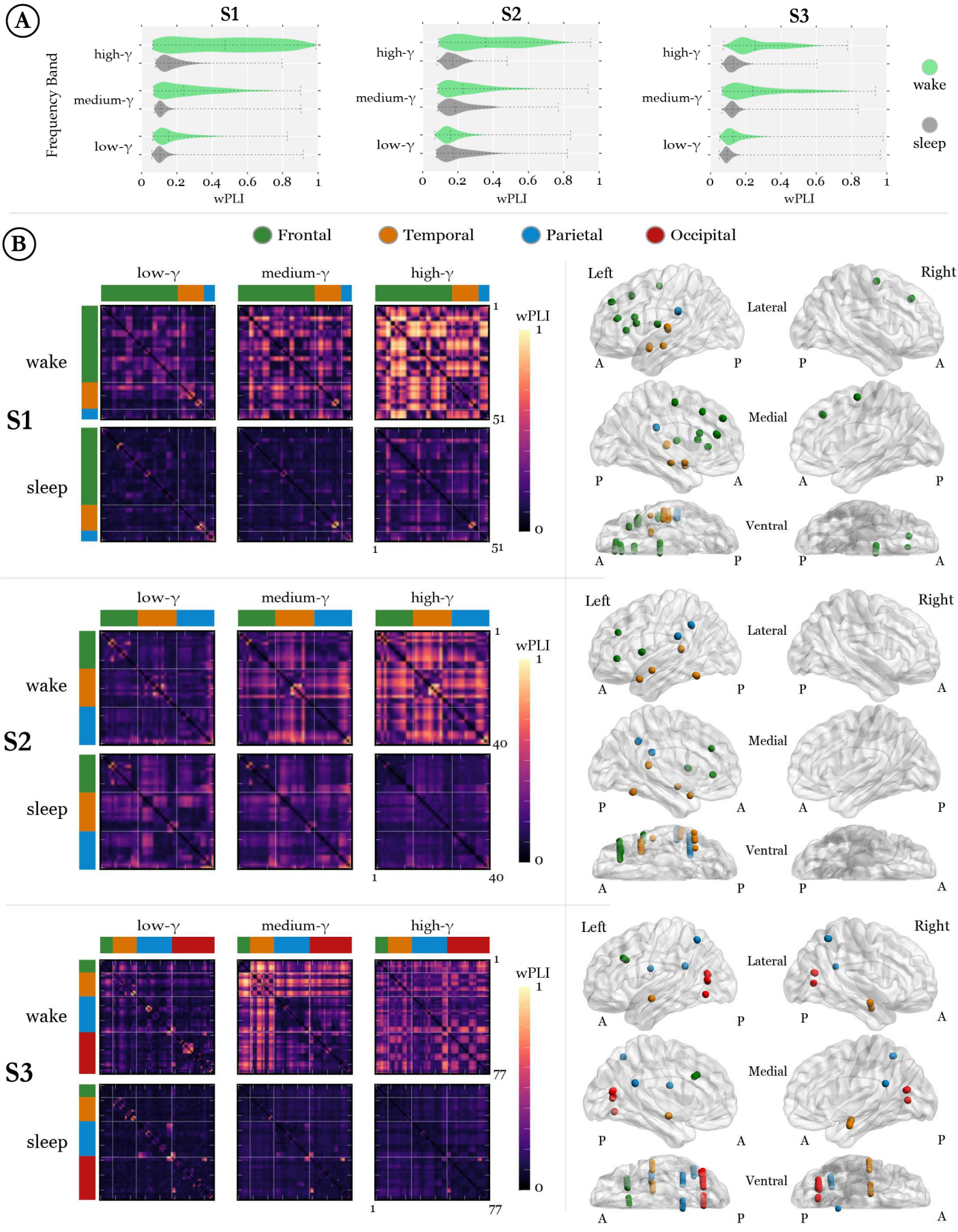

**Figure 2. Connectivity analysis results for each subject, condition and frequency band.** A) Violin plot of wPLI distributions. Vertical dotted lines indicate extremes and median. Vertical axes correspond to frequency bands and horizontal axes to wPLI values. B) *Left*: channel-by-channel matrix representation of wPLI values. Vertical and horizontal axes represent electrodes, ordered and color-coded by lobe. Colormap indicates wPLI values. Within-subject top panels indicate wake condition and bottom panels indicate sleep condition. *Right:* Electrode location by subject, color-coded by lobe. wPLI: weighted Phase Lag Index.

Pearson's correlation coefficients of wPLI values and Euclidean distance between contacts (Figure 3) showed that wPLI estimates were not driven by local interactions ($\bar{x}$ $r$ = 0.01, σ $r$ = 0.05, min $r$ = -0.07, max $r$ = 0.12; across all subjects, conditions and frequency bands; see also Supplementary Figure SF2).

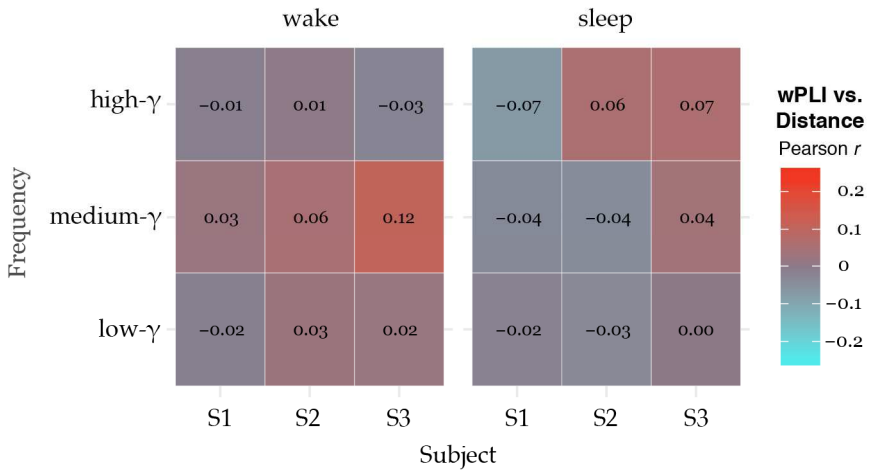


**Figure 3. Connectivity vs. distance correlation matrix.** Pearson's correlation coefficient between connectivity values and Euclidean distance for each subject, condition and frequency band.

Results of the network-based analysis are summarized in Figure 4. Within the γ-range, the high-γ band was the only one to show differences between conditions on the three subjects (Figure 4A). The consistently increased connectivity during wakefulness that we found in the high-γ band did not occur in other frequency bands, thus confirming the specificity of the effect (Figure 4B; see also Supplementary Figure SF1). Interestingly, the high-α band showed increased connectivity during sleep across the three subjects.

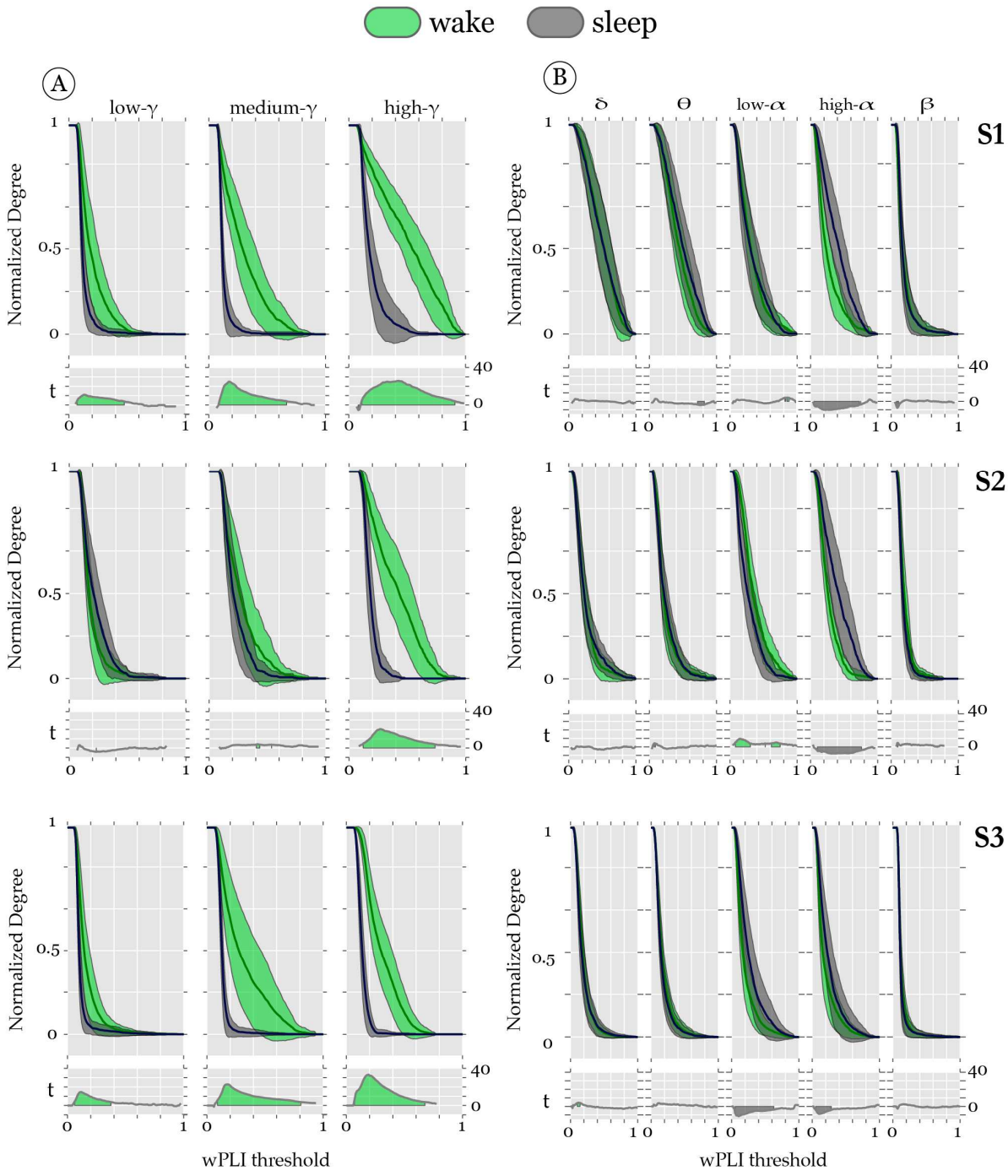


**Figure 4. Network-based analysis.** *Upper panels*. Normalized mean degree (lines) and standard deviation (shades) as a function of thresholding value. *Lower panels*. Welch *t*-value as a function of threshold. Shaded area represents $p < .05$ after correction for multiple comparisons. Color represents condition with higher mean. Within-subject panels correspond to frequency bands. wPLI: weighted Phase Lag Index. A) Results for the γ-range. B) Results for the remaining canonical frequency bands.

In order to test if connectivity differences were associated with differences in power we compared it between conditions for each frequency band of interest (Figure 5). Power was significantly higher during wakefulness than during sleep in the three

sub-bands of the γ-range for S1 (low: $p_n$ < .001; medium: $p_n$ < .001; high: $p_n$ < .001) and S2 (low: $p_n$ < .001; medium: $p_n$ < .001; high: $p_n$ < .001). Interestingly, in S3, it was higher during sleep in the low-γ band ($p_n$ < .001) and the difference was not significant in the medium and high-γ bands (medium: $p_n$ = 0.360; high: $p_n$ = 0.058).

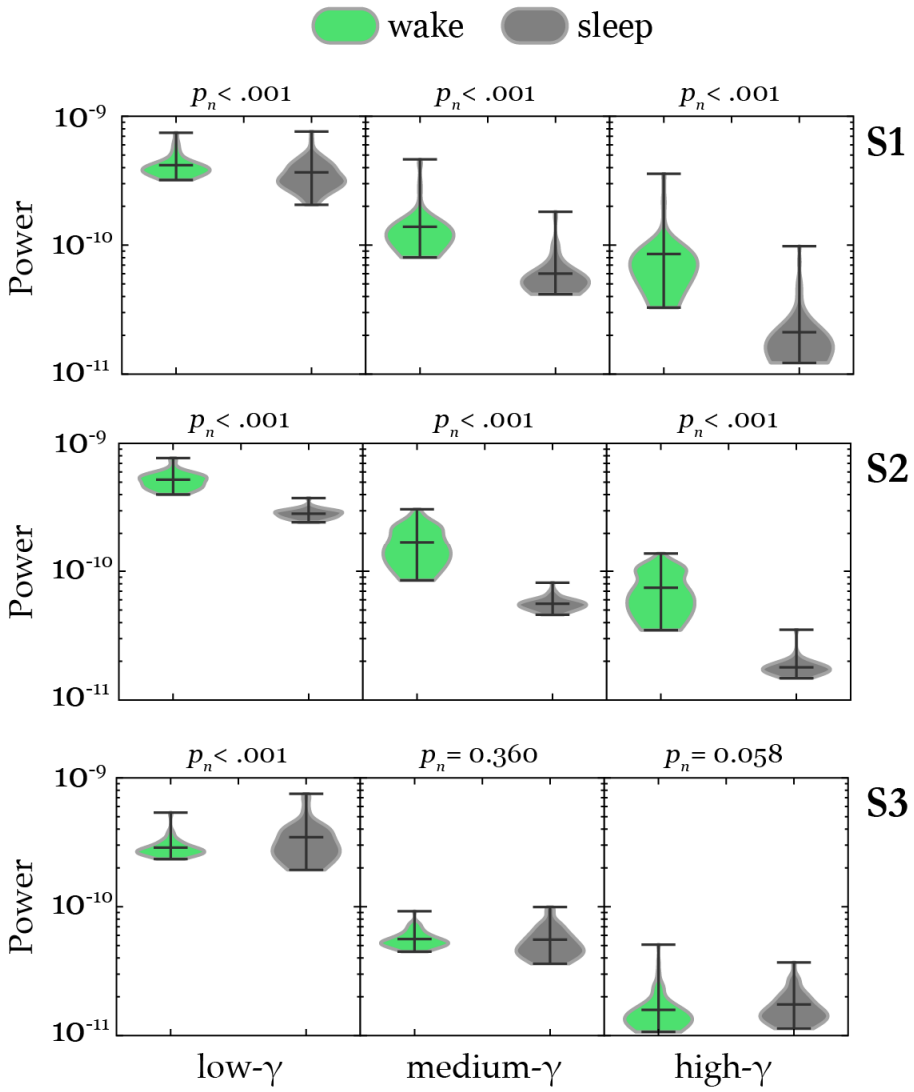


**Figure 5. Power analysis.** Violin plots of the power estimates for each subject and frequency band. Horizontal lines represent extremes and mean of the distributions. $p_n$: p-value based on the number of suprathreshold permutation tests, corrected for multiple comparisons using the Holm-Bonferroni method.

The electrode-based analysis showed that the model with high-γ obtained the best goodness-of-fit score (QIC, lower values indicate better fit) and that its only significant predictor was high-γ mean-wPLI (Table 1). In other words, high-γ

connectivity discriminated between states better than any other canonical frequency band and none of the epileptic activity indexes, nor their interactions with high-γ, were statistically significant. Distributions and logistic curve for the high-γ predictor are illustrated in Figure 6. VIFs showed that collinearity was not an issue for the model (high-γ: 1.22, ripples: 1.01, spikes: 1.23).

Ⓐ

| | Estimate | Std. Err. | Wald | *p* |
|---|---|---|---|---|
| intercept | -13.15 | 3.44 | 14.59 | 0.0001*** |
| high-γ | 51.42 | 14.12 | 13.29 | 0.0002*** |
| ripples | 14.31 | 10.55 | 1.84 | 0.17 |
| spikes | -7.24 | 11.40 | 0.40 | 0.52 |
| high-γ : ripples | -43.52 | 59.53 | 0.53 | 0.46 |
| high-γ : spikes | 65.95 | 83.16 | 0.62 | 0.42 |
| ripples : spikes | -20.19 | 45.73 | 0.19 | 0.65 |
| high-γ : ripples : spikes | -24.97 | 323.63 | 0.006 | 0.93 |

Ⓑ

| | Band | QIC |
|---|---|---|
| 1 | high-γ | 92.6 |
| 2 | medium-γ | 218.4 |
| 3 | high-α | 240.3 |
| 4 | θ | 248.5 |
| 5 | δ | 260.1 |
| 6 | β | 315.2 |
| 7 | low-α | 344.6 |
| 8 | low-γ | 483.4 |

**Table 1. Generalized Estimating Equations analysis.** A) Estimates and significance tests of each predictor and their interactions for the model with high-γ connectivity. B) Ranking of goodness-of-fit of the models for each frequency band (lower values indicate better fit). QIC: quasi-likelihood under the independence model criterion. *** $p < .001$

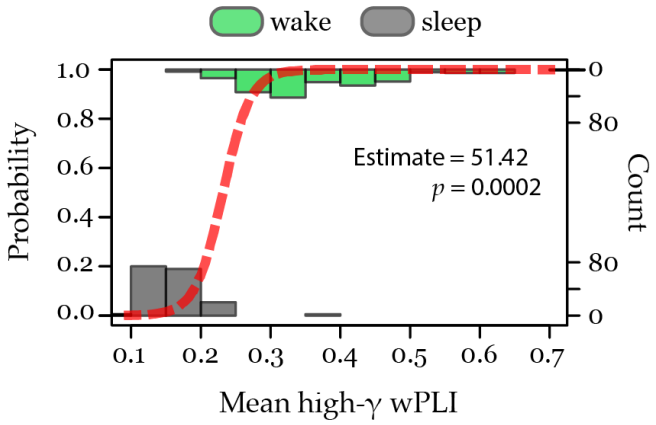


**Figure 6. Logistic curve of the high-γ predictor of the Generalized Estimating Equations model.** Histograms represent distribution of mean wPLI values for each condition. wPLI: weighted Phase Lag Index.

The high-γ band showed the larger and more consistent effect across subjects and analyses. Consequently, region-based *post hoc* statistical analyses were restricted to this specific frequency band. Both the spatial distribution of mean-wPLI values and the region-based analyses indicate that connectivity was lower during sleep in almost all sampled areas (Figures 7 to 9; see also Supplementary Figures SF3 and SF4 for the spatial profile of the lower frequency bands). Interestingly, during wakefulness, subjects showed different spatial profiles. S1 exhibited higher values in electrodes located in frontal areas, S2 in temporal regions, and S3 presented a more homogeneous pattern.

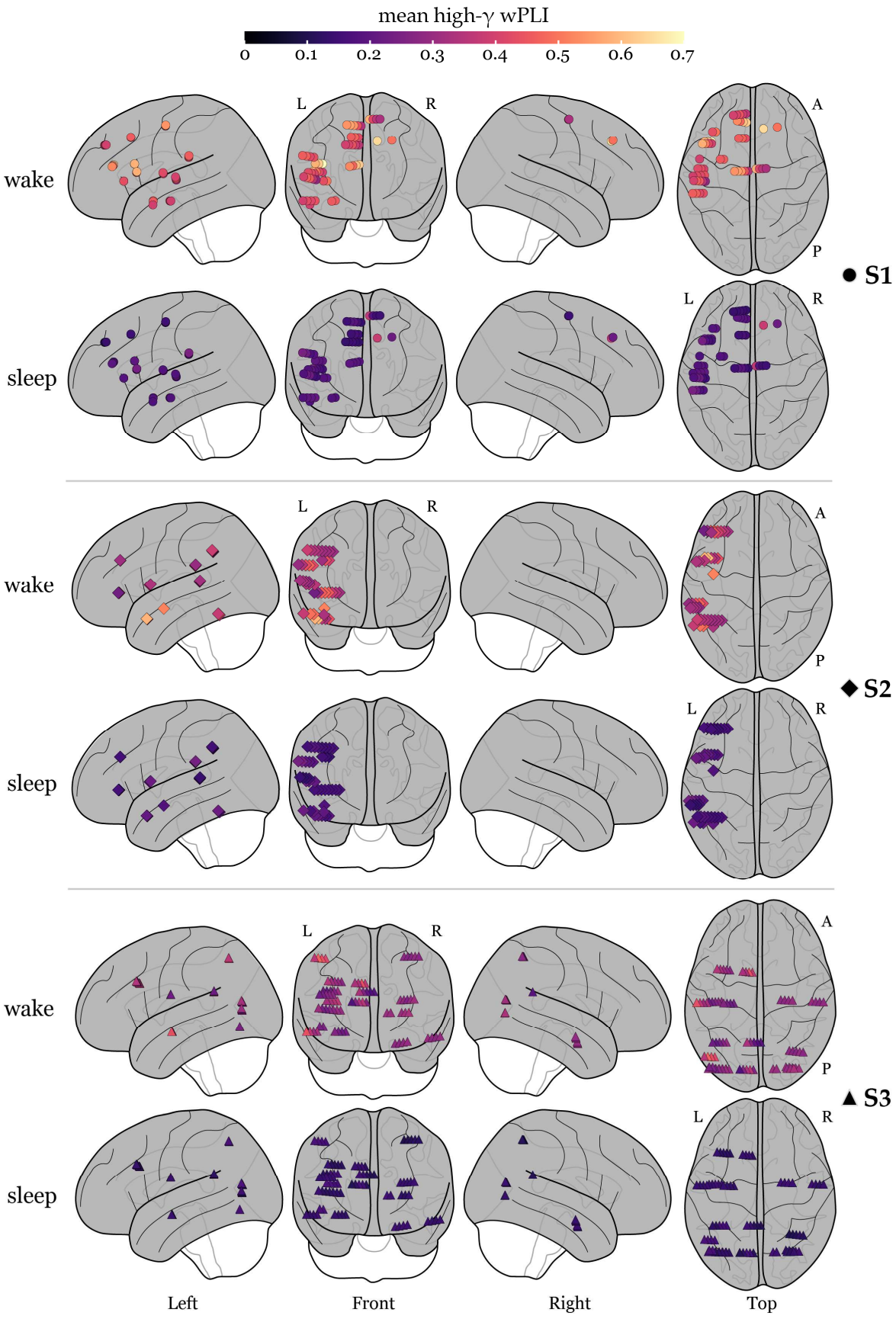


**Figure 7. Electrode location and mean high-γ wPLI for each subject.** Within-subject *top* and *bottom* panels correspond to wake and sleep conditions respectively. Color represents mean wPLI values and symbols denote subjects. wPLI: weighted Phase Lag Index.

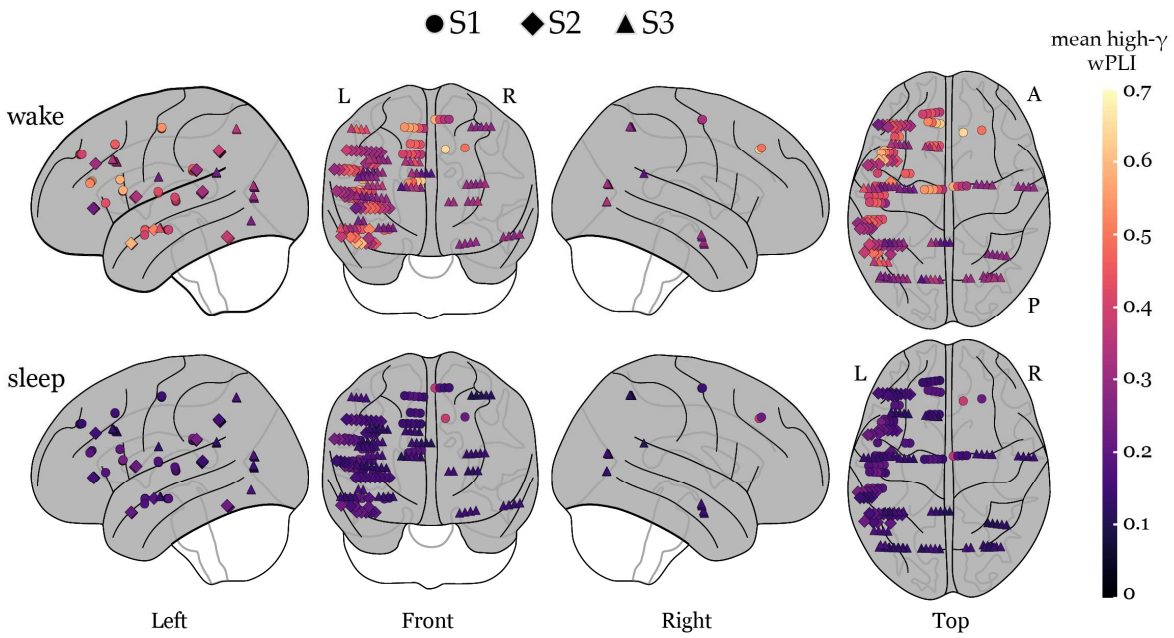


**Figure 8. Combined electrode location and mean high-γ wPLI.** *Top* and *bottom* panels correspond to wake and sleep conditions respectively. Color represents mean wPLI values and symbols denote subjects. wPLI: weighted Phase Lag Index.

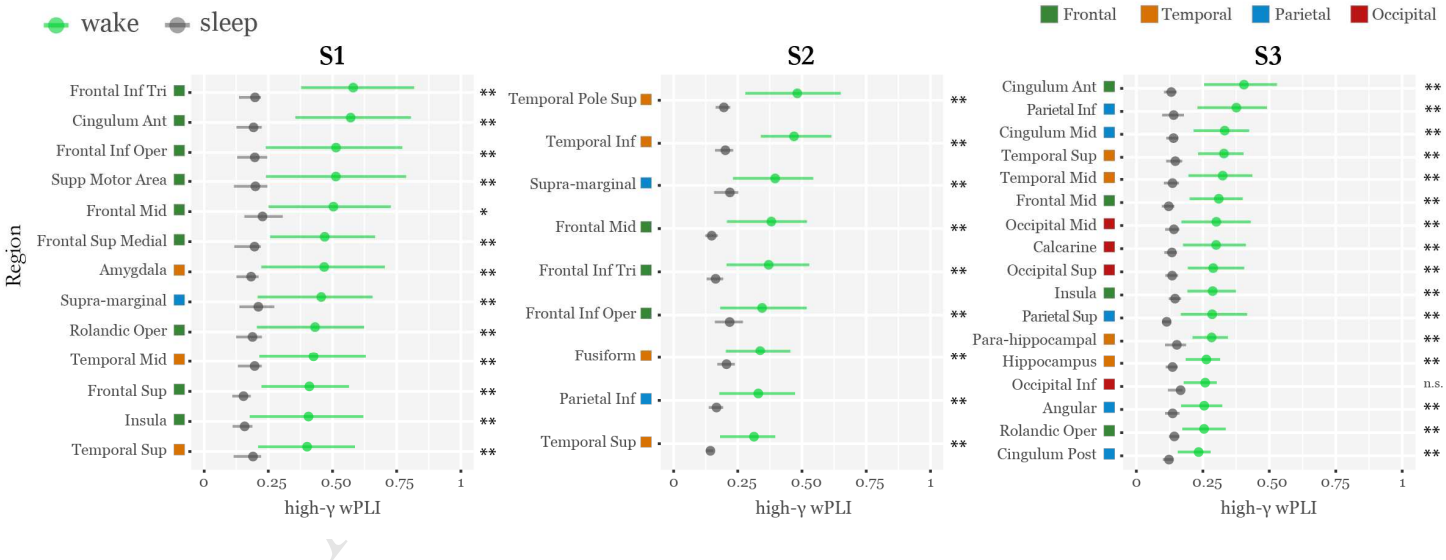


**Figure 9. High-γ wPLI by anatomical region for each subject.** Circles represent mean-wPLI value and lines represent Inter Quartile Range (IQR). Areas are shown in descending order of mean wPLI in the *wake* condition. Squares' colours represent corresponding brain lobes of anatomical regions. Asterisks denote statistical significance (corrected for multiple comparisons). Region names follow the Automated Anatomical Labeling naming-convention. Frontal Inf Tri: inferior frontal gyrus pars triangularis; Cingulum Ant: anterior cingulate gyrus; Frontal Inf Oper:

inferior frontal gyrus pars opercularis; Supp Motor Area: supplementary motor area; Frontal Mid: middle frontal gyrus; Frontal Sup Medial: superior frontal gyrus medial part; Supra-marginal: supramarginal gyrus; Rolandic Oper: rolandic operculum; Temporal Mid: middle temporal gyrus; Frontal Sup: superior frontal gyrus; Temporal Sup: superior temporal gyrus; Temporal Pole Sup: superior temporal pole; Temporal Inf: inferior temporal gyrus; Fusiform: fusiform gyrus; Parietal Inf: inferior parietal lobule; Cingulum Mid: middle cingulate gyrus; Occipital Mid: middle occipital gyrus; Calcarine: calcarine sulcus; Occipital Sup: superior occipital gyrus; Parietal Sup: superior parietal lobule; Para-hippocampal: parahippocampal gyrus; Occipital Inf: inferior occipital gyrus; Angular: angular gyrus; Cingulum Post: posterior cingulate gyrus; wPLI: weighted Phase Lag Index; n.s.: non-significant (alpha-level: 0.05); * $p < .01$; ** $p < .001$

## 4. Discussion

Our study was the first to test medium-γ (60-90 Hz) and high-γ (> 90 Hz) connectivity differences between wakefulness and sleep at both local and distant areas. Results showed that connectivity in the high-γ band (or ε-band) was higher in the wake state and consistently differentiated between conditions in all the analyses performed. Moreover, our results showed that these connectivity differences were not driven by local interactions, nor by differences in epileptiform activity between states. Furthermore, connectivity differences existed even when high-γ power was not significantly different between conditions (S3).

Contemporary accounts of consciousness, such as Integrated Information Theory (IIT; Tononi and Massimini, 2008) and Global Neuronal Workspace Theory (GNWT; Dehaene and Changeux, 2005; Dehaene and Changeux, 2011), consider information integration across brain regions as a fundamental process. Our results are, in principle, in line with both of them as they show that interregional high-γ synchrony, one of the putative mechanisms of brain communication (Buzsaki and Schomburg, 2015), is higher during wakefulness than during sleep. However, different theories ascribe dissimilar importance to the role of specific brain regions in the emergence of consciousness. The main anatomical postulates of GNWT are that long-distance cortical

networks are fundamental for conscious processing, with crucial contributions of the prefrontal, parieto-temporal and cingulate cortices (Dehaene and Changeux, 2011). The importance given to the parietal and prefrontal cortices is also congruent with other theories of consciousness, as Dynamic Core and Causal Density theories (Bor and Seth, 2012). IIT, on the other hand, does not assign any particular role to the aforementioned areas. Instead, it defines the physical substrate of consciousness in terms of cause-effect power (Tononi et al., 2016). Interestingly, our results indicate the frontal, cingulate and parietal cortices were among the mostly connected areas, but they also show that in one subject the temporal cortex was the most connected region, even though frontal and parietal areas were also sampled. Whichever the case may be, the small number of subjects in our study, combined with the partial brain coverage of intracranial recordings, undermines any conclusion regarding the role of specific regions. Future studies combining a large number of subjects will be required to delve into the matter.

Neural synchrony in the γ-range, by itself, has been proposed as being crucial for consciousness (Cavinato et al., 2015; Engel and Singer, 2001; Melloni et al., 2007; Varela et al., 2001). Our results showed that the high-γ band differentiated between states better than any other canonical frequency band and that it was the only sub-band of the γ-range that consistently showed differences in all analyses across all subjects. Interestingly, however, some pairs of adjacent or within-lobe contacts showed relatively high connectivity values in the γ-range during sleep, suggesting some degree of preserved local γ-synchrony.

A growing body of literature indicates that LFP-measured high-γ activity constitutes a reliable index of multiunit activity, that is, an index of spiking activity in the vicinity of the electrode (Crone et al., 2001; Edwards et al., 2009; Jenison et al., 2015; Miller et al., 2014; Ray et al., 2008; Ray and Maunsell, 2011; Steinschneider et al., 2008; Tang et al., 2017). Consequently, the specificity of the high-γ band observed our study could be attributed to synchrony differences between wakefulness and sleep at

the aforementioned hierarchical level of physiological activity. However, a comprehensive analysis of spiking activity (Rasch et al., 2008) is beyond the scope and methodological capability of our study, and it should therefore be pursued in future investigations.

Importantly, the difference between wakefulness and sleep is not circumscribed to the conscious global state but also includes differences in other domains, such as attention (Koch et al., 2016). Synchronization in the γ-range has been shown to play a role in memory (Fell et al., 2001; Sederberg et al., 2007), attention (Fries et al., 2001), and sensory integration (Ghazanfar et al., 2008; Maier et al., 2004), among many other domains (for a review see, Wang, 2010). Therefore, even though our results are in line with the hypothesis of the role of γ-synchrony in consciousness, other confounding factors cannot be ruled out. However, the relationship between consciousness and the mentioned domains is far from being clear (Dehaene et al., 2006; Graziano and Kastner, 2011; Koch and Tsuchiya, 2007). The entanglement of consciousness with other brain processes is an intrinsic limitation of studies investigating levels of consciousness. Converging evidence from multiple experimental designs will be required to overcome this limitation and decide on the role that phase-relationships play in the emergence of consciousness on the brain.

We also found increased connectivity during sleep in the high-α band. This result could have been caused by sleep spindles (Sakellariou et al., 2016). However, synchrony and propagation of sleep spindles are still a matter of debate (Andrillon et al., 2011; Frauscher et al., 2015; Souza et al., 2016). Moreover, the role of α-synchronization in brain dynamics is also a matter of discussion, as it has been shown to be associated with both suppression of communication and active information processing (Palva and Palva, 2007, 2011). An in depth discussion of this finding is beyond the scope of the present article. Future studies will be required to replicate this finding, test its relationship with sleep spindles and discuss its theoretical significance.

Brain signals in the higher range of the γ-band can only be reliably measured in humans via intracranial recordings; this restriction can explain the controversies found using other techniques that lack the spectral extension of iEEG. For example, increased EEG γ-synchrony during propofol-induced loss of consciousness (Murphy et al., 2011) could be possibly explained by confounding factors of the technique, as miniature saccades (Fries et al., 2008; Yuval-Greenberg et al., 2008) and muscle artifacts (Muthukumaraswamy, 2013; Walder et al., 2002). Furthermore, EEG and MEG signals are prone to distortions because of the skull and intermediate tissue between sources and sensors (Buzsaki et al., 2012). In our study, any substantial influence of these possible confounds was unlikely because we used a non-zero phase lag measure of connectivity, which is robust against muscular and ocular artifacts, and iEEG, which records direct brain activity.

Previous studies that compared synchrony in the γ-range between wakefulness and sleep used "coherence" as the connectivity measure (Bullock et al., 1995; Cantero et al., 2004). This approach, besides measuring the consistency of the phase difference between oscillations from different sources, is sensitive to volume conduction, common pick-up, and common references (Bastos and Schoffelen, 2015; Cohen, 2014). These three problems, which are instantaneous within current measurement capabilities, produce spurious connectivity at 0 or 180º phase differences. Even though volume conduction is less problematic in iEEG than in scalp EEG, it cannot be considered irrelevant (Herreras, 2016). Besides, when measuring iEEG γ-connectivity, an often-neglected artifactual source of synchrony is volume-conducted head and neck muscular activity, which also produces spurious connectivity at 0 or 180º (Buzsaki and Schomburg, 2015; Kovach et al., 2011). Therefore, connectivity measures that do not take into account 0 and 180º phase differences provide more reliable estimates. In our case we used the wPLI (Vinck et al., 2011), which is weighted by the distance from 0 and 180º and therefore overcomes the limitations of previous studies (see Equation 2).

Bullock et al. (1995) found no differences between wakefulness and sleep, but their analysis was restricted to adjacent electrodes and focused on the fluctuation of coherence values. They also found that results were positively correlated between frequency bands. Our results showed that the high-γ and high-α bands differentiated between conditions and that high-γ was higher during wakefulness whilst high-α was higher during sleep. Cantero et al. (2004) showed that within- and between-regional γ-coherence (35-58 Hz) was higher during wakefulness. Our results showed that in two out of three subjects the low-γ band (30-60 Hz) differentiated between conditions, and the high-γ band (90-120 Hz) in all subjects. In addition, our results exhibited that high connectivity values were present both within and between regions. Consequently, our results are in line with the findings of Cantero et al. (2004) and contrast with those obtained by Bullock et al. (1995).

Power in the ranges of 50-90 and 90-150 Hz are thought to be generated by different physiological mechanisms (Belluscio et al., 2012; Buzsaki and Wang, 2012). Our results showed that connectivity differences between conditions were not homogeneous within sub-bands of the γ-range. Consequently, future studies should consider discriminating this frequency bands in the search for neural correlates of global conscious states.

In sum, our results constitute the first demonstration of high-γ connectivity differences between wakefulness and sleep at both local and distant sites. They are in line with the most influential contemporary theories of consciousness, as they showed that interregional communication is higher during wakeful consciousness than during sleep, and that this effect was restricted to the γ-range. Finally, they also provide insights about the cerebral dynamics of the sleep-wake cycle.

## 5. Limitations and further research

Our study is not without limitations. First, we could not score sleep stages as the experiment's clinical set-up precluded hypnogram recordings. However, we discriminated between wakefulness and sleep using the robust DA measure, which has been validated against other conventional scoring methods and successfully used in previous iEEG research (Magnin et al., 2010). Future studies could use simultaneous iEEG-EEG-EOG-EMG to establish more precise distinctions of sleep stages and investigate connectivity differences among them. Second, use of the iEEG technique offered only limited spatial coverage of the participants' brains. However, results proved consistent across subjects even though the spatial distribution of the electrodes varied among them. Collaborative efforts from multiple laboratories will be required to gather enough information in order to achieve a relatively large between-subject spatial coverage. Finally, present results include a caveat, as they are derived from epileptic patients and may not accurately represent a healthy population. To account for it we controlled for relevant factors. Intracranial recordings typically include both pathological and non-pathological brain regions (Engel et al., 2005). We addressed this issue by: (i) excluding channels in epileptic foci regions, (ii) using stringent inclusion criteria for the remaining channels (see Materials & Methods), (iii) carefully inspecting MRI scans to rule out structural abnormalities, and (iv) testing the difference between conditions including subtler epileptic activity, by incorporating automatically detected ripples and spikes in the analyses (GEE models). It is again a trade-off of the iEEG technique which counterweights its limitations by providing the best spatiotemporal resolution currently available in humans. For a discussion of the last two mentioned limitations see (Lachaux et al., 2003).

## 6. Conclusion

The role of γ-synchrony in consciousness and cognition constitutes a matter or ardent debate. Our study showed, for the first time, that wakefulness and sleep are selectively

differentiated by high-γ connectivity at both short and long distances. This was achieved via a state-of-the-art connectivity measure that overcomes limitations of previous works. Previous studies lacking the spectral resolution of iEEG should be interpreted cautiously in their claims about the role of γ-synchrony in consciousness. Our study also showed that results were not homogeneous across sub-bands of the γ-range and therefore, in line with physiologically grounded recommendations (Buzsaki and Wang, 2012), future investigations should consider separating them. Our findings provide evidence in line with contemporary theories of consciousness and also contribute to understanding the cerebral dynamics of the sleep-wake cycle.

**References**

Aarts, E., Verhage, M., Veenvliet, J.V., Dolan, C.V., van der Sluis, S., 2014. A solution to dependency: using multilevel analysis to accommodate nested data. Nat Neurosci 17, 491-496.

Abraham, A., Pedregosa, F., Eickenberg, M., Gervais, P., Mueller, A., Kossaifi, J., Gramfort, A., Thirion, B., Varoquaux, G., 2014. Machine learning for neuroimaging with scikit-learn. Front Neuroinform 8, 14.

Acharya, U.R., Faust, O., Kannathal, N., Chua, T., Laxminarayan, S., 2005. Non-linear analysis of EEG signals at various sleep stages. Comput Methods Programs Biomed 80, 37-45.

Achermann, P., Hartmann, R., Gunzinger, A., Guggenbuhl, W., Borbely, A.A., 1994. Correlation dimension of the human sleep electroencephalogram: cyclic changes in the course of the night. Eur J Neurosci 6, 497-500.

Andrillon, T., Nir, Y., Staba, R.J., Ferrarelli, F., Cirelli, C., Tononi, G., Fried, I., 2011. Sleep spindles in humans: insights from intracranial EEG and unit recordings. J Neurosci 31, 17821-17834.

Bastos, A.M., Schoffelen, J.M., 2015. A Tutorial Review of Functional Connectivity Analysis Methods and Their Interpretational Pitfalls. Front Syst Neurosci 9, 175.

Bayne, T., Hohwy, J., Owen, A.M., 2016. Are There Levels of Consciousness? Trends in Cognitive Sciences.

Belluscio, M.A., Mizuseki, K., Schmidt, R., Kempter, R., Buzsaki, G., 2012. Cross-frequency phase-phase coupling between theta and gamma oscillations in the hippocampus. J Neurosci 32, 423-435.

Bor, D., Seth, A.K., 2012. Consciousness and the prefrontal parietal network: insights from attention, working memory, and chunking. Front Psychol 3, 63.

Bullmore, E., Sporns, O., 2009. Complex brain networks: graph theoretical analysis of structural and functional systems. Nat Rev Neurosci 10, 186-198.

Bullock, T.H., McClune, M.C., Achimowicz, J.Z., Iragui-Madoz, V.J., Duckrow, R.B., Spencer, S.S., 1995. Temporal fluctuations in coherence of brain waves. Proc Natl Acad Sci U S A 92, 11568-11572.

Buzsáki, G., 2006. Rhythms of the brain. Oxford University Press, Oxford ; New York.
Buzsaki, G., Anastassiou, C.A., Koch, C., 2012. The origin of extracellular fields and currents--EEG, ECoG, LFP and spikes. Nat Rev Neurosci 13, 407-420.
Buzsaki, G., Schomburg, E.W., 2015. What does gamma coherence tell us about inter-regional neural communication? Nat Neurosci 18, 484-489.
Buzsaki, G., Wang, X.J., 2012. Mechanisms of gamma oscillations. Annu Rev Neurosci 35, 203-225.
Canales-Johnson, A., Silva, C., Huepe, D., Rivera-Rei, A., Noreika, V., Garcia Mdel, C., Silva, W., Ciraolo, C., Vaucheret, E., Sedeno, L., Couto, B., Kargieman, L., Baglivo, F., Sigman, M., Chennu, S., Ibanez, A., Rodriguez, E., Bekinschtein, T.A., 2015. Auditory Feedback Differentially Modulates Behavioral and Neural Markers of Objective and Subjective Performance When Tapping to Your Heartbeat. Cereb Cortex 25, 4490-4503.
Cantero, J.L., Atienza, M., Madsen, J.R., Stickgold, R., 2004. Gamma EEG dynamics in neocortex and hippocampus during human wakefulness and sleep. NeuroImage 22, 1271-1280.
Cavinato, M., Genna, C., Manganotti, P., Formaggio, E., Storti, S.F., Campostrini, S., Arcaro, C., Casanova, E., Petrone, V., Piperno, R., Piccione, F., 2015. Coherence and Consciousness: Study of Fronto-Parietal Gamma Synchrony in Patients with Disorders of Consciousness. Brain Topogr 28, 570-579.
Chen, J., Dastjerdi, M., Foster, B.L., LaRocque, K.F., Rauschecker, A.M., Parvizi, J., Wagner, A.D., 2013. Human hippocampal increases in low-frequency power during associative prediction violations. Neuropsychologia 51, 2344-2351.
Chennu, S., Finoia, P., Kamau, E., Allanson, J., Williams, G.B., Monti, M.M., Noreika, V., Arnatkeviciute, A., Canales-Johnson, A., Olivares, F., Cabezas-Soto, D., Menon, D.K., Pickard, J.D., Owen, A.M., Bekinschtein, T.A., 2014. Spectral signatures of reorganised brain networks in disorders of consciousness. PLoS Comput Biol 10, e1003887.
Chennu, S., Noreika, V., Gueorguiev, D., Blenkmann, A., Kochen, S., Ibanez, A., Owen, A.M., Bekinschtein, T.A., 2013. Expectation and attention in hierarchical auditory prediction. J Neurosci 33, 11194-11205.
Chennu, S., O'Connor, S., Adapa, R., Menon, D.K., Bekinschtein, T.A., 2016. Brain Connectivity Dissociates Responsiveness from Drug Exposure during Propofol-Induced Transitions of Consciousness. PLoS Comput Biol 12, e1004669.
Clemens, Z., Janszky, J., Szucs, A., Bekesy, M., Clemens, B., Halasz, P., 2003. Interictal epileptic spiking during sleep and wakefulness in mesial temporal lobe epilepsy: a comparative study of scalp and foramen ovale electrodes. Epilepsia 44, 186-192.
Cohen, M.X., 2014. Analyzing neural time series data : theory and practice. The MIT Press, Cambridge, Massachusetts.
Crone, N.E., Boatman, D., Gordon, B., Hao, L., 2001. Induced electrocorticographic gamma activity during auditory perception. Brazier Award-winning article, 2001. Clin Neurophysiol 112, 565-582.
De Gennaro, L., Ferrara, M., 2003. Sleep spindles: an overview. Sleep Med Rev 7, 423-440.
Dehaene, S., Changeux, J.P., 2005. Ongoing spontaneous activity controls access to consciousness: a neuronal model for inattentional blindness. PLoS Biol 3, e141.
Dehaene, S., Changeux, J.P., 2011. Experimental and theoretical approaches to conscious processing. Neuron 70, 200-227.
Dehaene, S., Changeux, J.P., Naccache, L., Sackur, J., Sergent, C., 2006. Conscious, preconscious, and subliminal processing: a testable taxonomy. Trends Cogn Sci 10, 204-211.

Dehaene, S., Naccache, L., 2001. Towards a cognitive neuroscience of consciousness: basic evidence and a workspace framework. Cognition 79, 1-37.
Delorme, A., Makeig, S., 2004. EEGLAB: an open source toolbox for analysis of single-trial EEG dynamics including independent component analysis. J Neurosci Methods 134, 9-21.
Edwards, E., Soltani, M., Kim, W., Dalal, S.S., Nagarajan, S.S., Berger, M.S., Knight, R.T., 2009. Comparison of time-frequency responses and the event-related potential to auditory speech stimuli in human cortex. J Neurophysiol 102, 377-386.
El-Baz, A.S., Acharya U, R., Laine, A., Suri, J.S., 2011. Multi modality state-of-the-art medical image segmentation and registration methodologies. Springer, New York.
Engel, A.K., Moll, C.K., Fried, I., Ojemann, G.A., 2005. Invasive recordings from the human brain: clinical insights and beyond. Nat Rev Neurosci 6, 35-47.
Engel, A.K., Singer, W., 2001. Temporal binding and the neural correlates of sensory awareness. Trends Cogn Sci 5, 16-25.
Engel, J., Jr., 2005. The emergence of neurosurgical approaches to the treatment of epilepsy. In: Waxman, S.G. (Ed.), From Neuroscience to Neurology: Neuroscience, Molecular Medicine, and the Therapeutic Transformation in Neurology. Elsevier, Amsterdam, pp. 81-105.
Fedorov, A., Beichel, R., Kalpathy-Cramer, J., Finet, J., Fillion-Robin, J.C., Pujol, S., Bauer, C., Jennings, D., Fennessy, F., Sonka, M., Buatti, J., Aylward, S., Miller, J.V., Pieper, S., Kikinis, R., 2012. 3D Slicer as an image computing platform for the Quantitative Imaging Network. Magn Reson Imaging 30, 1323-1341.
Fell, J., Klaver, P., Lehnertz, K., Grunwald, T., Schaller, C., Elger, C.E., Fernandez, G., 2001. Human memory formation is accompanied by rhinal-hippocampal coupling and decoupling. Nat Neurosci 4, 1259-1264.
Fell, J., Ludowig, E., Rosburg, T., Axmacher, N., Elger, C.E., 2008. Phase-locking within human mediotemporal lobe predicts memory formation. NeuroImage 43, 410-419.
Fell, J., Roschke, J., Mann, K., Schaffner, C., 1996. Discrimination of sleep stages: a comparison between spectral and nonlinear EEG measures. Electroencephalogr Clin Neurophysiol 98, 401-410.
Frauscher, B., von Ellenrieder, N., Dubeau, F., Gotman, J., 2015. Scalp spindles are associated with widespread intracranial activity with unexpectedly low synchrony. NeuroImage 105, 1-12.
Fries, P., 2009. Neuronal gamma-band synchronization as a fundamental process in cortical computation. Annu Rev Neurosci 32, 209-224.
Fries, P., Reynolds, J.H., Rorie, A.E., Desimone, R., 2001. Modulation of oscillatory neuronal synchronization by selective visual attention. Science 291, 1560-1563.
Fries, P., Scheeringa, R., Oostenveld, R., 2008. Finding gamma. Neuron 58, 303-305.
Gardner, A.B., Worrell, G.A., Marsh, E., Dlugos, D., Litt, B., 2007. Human and automated detection of high-frequency oscillations in clinical intracranial EEG recordings. Clin Neurophysiol 118, 1134-1143.
Ghazanfar, A.A., Chandrasekaran, C., Logothetis, N.K., 2008. Interactions between the superior temporal sulcus and auditory cortex mediate dynamic face/voice integration in rhesus monkeys. J Neurosci 28, 4457-4469.
Goupil, L., Bekinschtein, T.A., 2012. Cognitive processing during the transition to sleep. Arch Ital Biol 150, 140-154.
Gramfort, A., Luessi, M., Larson, E., Engemann, D.A., Strohmeier, D., Brodbeck, C., Goj, R., Jas, M., Brooks, T., Parkkonen, L., Hamalainen, M., 2013. MEG and EEG data analysis with MNE-Python. Front Neurosci 7, 267.
Gramfort, A., Luessi, M., Larson, E., Engemann, D.A., Strohmeier, D., Brodbeck, C., Parkkonen, L., Hamalainen, M.S., 2014. MNE software for processing MEG and EEG data. NeuroImage 86, 446-460.

Graziano, M.S., Kastner, S., 2011. Human consciousness and its relationship to social neuroscience: A novel hypothesis. Cogn Neurosci 2, 98-113.
Hagberg, H., Schult, D.A., Swart, P.J., 2008. Exploring network structure, dynamics, and function using NetworkX. In: Varoquaux, G., Vaught, T., Millman, J. (Eds.), Proceedings of the 7th Python in Science Conference (SciPy2008), Pasadena, CA USA, pp. 11-15.
Herreras, O., 2016. Local Field Potentials: Myths and Misunderstandings. Front Neural Circuits 10, 101.
Hesse, E., Mikulan, E., Decety, J., Sigman, M., Garcia Mdel, C., Silva, W., Ciraolo, C., Vaucheret, E., Baglivo, F., Huepe, D., Lopez, V., Manes, F., Bekinschtein, T.A., Ibanez, A., 2016. Early detection of intentional harm in the human amygdala. Brain 139, 54-61.
Hohwy, J., 2009. The neural correlates of consciousness: new experimental approaches needed? Conscious Cogn 18, 428-438.
Holm, S., 1979. A Simple Sequentially Rejective Multiple Test Procedure. Scandinavian Journal of Statistics 6, 65-70.
Honey, C.J., Sporns, O., Cammoun, L., Gigandet, X., Thiran, J.P., Meuli, R., Hagmann, P., 2009. Predicting human resting-state functional connectivity from structural connectivity. Proc Natl Acad Sci U S A 106, 2035-2040.
Huettel, S.A., Song, A.W., McCarthy, G., 2014. Functional magnetic resonance imaging, Third edition. ed. Sinauer Associates, Inc., Publishers, Sunderland, Massachusetts, U.S.A.
Jacobs, J., Kahana, M.J., 2010. Direct brain recordings fuel advances in cognitive electrophysiology. Trends Cogn Sci 14, 162-171.
Jacobs, J., Staba, R., Asano, E., Otsubo, H., Wu, J.Y., Zijlmans, M., Mohamed, I., Kahane, P., Dubeau, F., Navarro, V., Gotman, J., 2012. High-frequency oscillations (HFOs) in clinical epilepsy. Prog Neurobiol 98, 302-315.
Jenison, R.L., Reale, R.A., Armstrong, A.L., Oya, H., Kawasaki, H., Howard, M.A., 3rd, 2015. Sparse Spectro-Temporal Receptive Fields Based on Multi-Unit and High-Gamma Responses in Human Auditory Cortex. PLoS ONE 10, e0137915.
Kabat, J., Krol, P., 2012. Focal cortical dysplasia - review. Pol J Radiol 77, 35-43.
Koch, C., Massimini, M., Boly, M., Tononi, G., 2016. Neural correlates of consciousness: progress and problems. Nature Reviews Neuroscience 17, 307-321.
Koch, C., Tsuchiya, N., 2007. Attention and consciousness: two distinct brain processes. Trends Cogn Sci 11, 16-22.
Kovach, C.K., Tsuchiya, N., Kawasaki, H., Oya, H., Howard, M.A., 3rd, Adolphs, R., 2011. Manifestation of ocular-muscle EMG contamination in human intracranial recordings. NeuroImage 54, 213-233.
Lachaux, J.P., Rudrauf, D., Kahane, P., 2003. Intracranial EEG and human brain mapping. J Physiol Paris 97, 613-628.
Le Van Quyen, M., Staba, R., Bragin, A., Dickson, C., Valderrama, M., Fried, I., Engel, J., 2010. Large-scale microelectrode recordings of high-frequency gamma oscillations in human cortex during sleep. J Neurosci 30, 7770-7782.
Magnin, M., Rey, M., Bastuji, H., Guillemant, P., Mauguiere, F., Garcia-Larrea, L., 2010. Thalamic deactivation at sleep onset precedes that of the cerebral cortex in humans. Proc Natl Acad Sci U S A 107, 3829-3833.
Maier, J.X., Neuhoff, J.G., Logothetis, N.K., Ghazanfar, A.A., 2004. Multisensory integration of looming signals by rhesus monkeys. Neuron 43, 177-181.
Maris, E., Oostenveld, R., 2007. Nonparametric statistical testing of EEG- and MEG-data. J Neurosci Methods 164, 177-190.
Mazziotta, J.C., Toga, A.W., Evans, A., Fox, P., Lancaster, J., 1995. A probabilistic atlas of the human brain: theory and rationale for its development. The International Consortium for Brain Mapping (ICBM). NeuroImage 2, 89-101.

Melloni, L., Molina, C., Pena, M., Torres, D., Singer, W., Rodriguez, E., 2007. Synchronization of neural activity across cortical areas correlates with conscious perception. J Neurosci 27, 2858-2865.
Miller, K.J., Honey, C.J., Hermes, D., Rao, R.P., denNijs, M., Ojemann, J.G., 2014. Broadband changes in the cortical surface potential track activation of functionally diverse neuronal populations. NeuroImage 85 Pt 2, 711-720.
Murphy, M., Bruno, M.A., Riedner, B.A., Boveroux, P., Noirhomme, Q., Landsness, E.C., Brichant, J.F., Phillips, C., Massimini, M., Laureys, S., Tononi, G., Boly, M., 2011. Propofol anesthesia and sleep: a high-density EEG study. Sleep 34, 283-291A.
Muthukumaraswamy, S.D., 2013. High-frequency brain activity and muscle artifacts in MEG/EEG: a review and recommendations. Front Hum Neurosci 7, 138.
Navarrete, M., Alvarado-Rojas, C., Le Van Quyen, M., Valderrama, M., 2016. RIPPLELAB: A Comprehensive Application for the Detection, Analysis and Classification of High Frequency Oscillations in Electroencephalographic Signals. PLoS ONE 11, e0158276.
O'brien, R.M., 2007. A Caution Regarding Rules of Thumb for Variance Inflation Factors. Quality & Quantity 41, 673-690.
Overgaard, M., Overgaard, R., 2010. Neural correlates of contents and levels of consciousness. Front Psychol 1, 164.
Palva, S., Palva, J.M., 2007. New vistas for alpha-frequency band oscillations. Trends Neurosci 30, 150-158.
Palva, S., Palva, J.M., 2011. Functional roles of alpha-band phase synchronization in local and large-scale cortical networks. Front Psychol 2, 204.
Pan, W., 2001. Akaike's information criterion in generalized estimating equations. Biometrics 57, 120-125.
Pereda, E., Gamundi, A., Nicolau, M.C., Rial, R., Gonzalez, J., 1999. Interhemispheric differences in awake and sleep human EEG: a comparison between non-linear and spectral measures. Neurosci Lett 263, 37-40.
Phipson, B., Smyth, G.K., 2010. Permutation P-values should never be zero: calculating exact P-values when permutations are randomly drawn. Stat Appl Genet Mol Biol 9, Article39.
Pittau, F., Megevand, P., Sheybani, L., Abela, E., Grouiller, F., Spinelli, L., Michel, C.M., Seeck, M., Vulliemoz, S., 2014. Mapping epileptic activity: sources or networks for the clinicians? Front Neurol 5, 218.
Pockett, S., Holmes, M.D., 2009. Intracranial EEG power spectra and phase synchrony during consciousness and unconsciousness. Conscious Cogn 18, 1049-1055.
R Core Team, 2015. R: A language and environment for statistical computing. R Foundation for Statistical Computing. Vienna, Austria. URL http://www.R-project.org/.
Rasch, M.J., Gretton, A., Murayama, Y., Maass, W., Logothetis, N.K., 2008. Inferring spike trains from local field potentials. J Neurophysiol 99, 1461-1476.
Ray, S., Crone, N.E., Niebur, E., Franaszczuk, P.J., Hsiao, S.S., 2008. Neural correlates of high-gamma oscillations (60-200 Hz) in macaque local field potentials and their potential implications in electrocorticography. J Neurosci 28, 11526-11536.
Ray, S., Maunsell, J.H., 2011. Different origins of gamma rhythm and high-gamma activity in macaque visual cortex. PLoS Biol 9, e1000610.
Rey, M., Bastuji, H., Garcia-Larrea, L., Guillemant, P., Mauguiere, F., Magnin, M., 2007. Human thalamic and cortical activities assessed by dimension of activation and spectral edge frequency during sleep wake cycles. Sleep 30, 907-912.
Rubinov, M., Sporns, O., 2010. Complex network measures of brain connectivity: uses and interpretations. NeuroImage 52, 1059-1069.
Sainani, K., 2010. The importance of accounting for correlated observations. PM R 2, 858-861.

Sakellariou, D., Koupparis, A.M., Kokkinos, V., Koutroumanidis, M., Kostopoulos, G.K., 2016. Connectivity Measures in EEG Microstructural Sleep Elements. Front Neuroinform 10, 5.
Sammaritano, M., Gigli, G.L., Gotman, J., 1991. Interictal spiking during wakefulness and sleep and the localization of foci in temporal lobe epilepsy. Neurology 41, 290-297.
Sederberg, P.B., Schulze-Bonhage, A., Madsen, J.R., Bromfield, E.B., McCarthy, D.C., Brandt, A., Tully, M.S., Kahana, M.J., 2007. Hippocampal and neocortical gamma oscillations predict memory formation in humans. Cereb Cortex 17, 1190-1196.
Shen, Y., Olbrich, E., Achermann, P., Meier, P.F., 2003. Dimensional complexity and spectral properties of the human sleep EEG. Electroencephalograms. Clin Neurophysiol 114, 199-209.
Souza, R.T., Gerhardt, G.J., Schonwald, S.V., Rybarczyk-Filho, J.L., Lemke, N., 2016. Synchronization and Propagation of Global Sleep Spindles. PLoS ONE 11, e0151369.
Stefan, H., Lopes da Silva, F.H., 2013. Epileptic neuronal networks: methods of identification and clinical relevance. Front Neurol 4, 8.
Steinschneider, M., Fishman, Y.I., Arezzo, J.C., 2008. Spectrotemporal analysis of evoked and induced electroencephalographic responses in primary auditory cortex (A1) of the awake monkey. Cereb Cortex 18, 610-625.
Tang, C., Hamilton, L.S., Chang, E.F., 2017. Intonational speech prosody encoding in the human auditory cortex. Science 357, 797-801.
Tao, J.X., Hawes-Ebersole, S., Baldwin, M., Shah, S., Erickson, R.K., Ebersole, J.S., 2009. The accuracy and reliability of 3D CT/MRI co-registration in planning epilepsy surgery. Clin Neurophysiol 120, 748-753.
Tononi, G., Boly, M., Massimini, M., Koch, C., 2016. Integrated information theory: from consciousness to its physical substrate. Nat Rev Neurosci 17, 450-461.
Tononi, G., Massimini, M., 2008. Why does consciousness fade in early sleep? Ann N Y Acad Sci 1129, 330-334.
Tzourio-Mazoyer, N., Landeau, B., Papathanassiou, D., Crivello, F., Etard, O., Delcroix, N., Mazoyer, B., Joliot, M., 2002. Automated anatomical labeling of activations in SPM using a macroscopic anatomical parcellation of the MNI MRI single-subject brain. NeuroImage 15, 273-289.
Uhlhaas, P.J., Pipa, G., Lima, B., Melloni, L., Neuenschwander, S., Nikolic, D., Singer, W., 2009. Neural synchrony in cortical networks: history, concept and current status. Front Integr Neurosci 3, 17.
Valderrama, M., Crepon, B., Botella-Soler, V., Martinerie, J., Hasboun, D., Alvarado-Rojas, C., Baulac, M., Adam, C., Navarro, V., Le Van Quyen, M., 2012. Human gamma oscillations during slow wave sleep. PLoS ONE 7, e33477.
Varela, F., Lachaux, J.P., Rodriguez, E., Martinerie, J., 2001. The brainweb: phase synchronization and large-scale integration. Nat Rev Neurosci 2, 229-239.
Vinck, M., Oostenveld, R., van Wingerden, M., Battaglia, F., Pennartz, C.M., 2011. An improved index of phase-synchronization for electrophysiological data in the presence of volume-conduction, noise and sample-size bias. NeuroImage 55, 1548-1565.
Walder, B., Tramer, M.R., Seeck, M., 2002. Seizure-like phenomena and propofol: a systematic review. Neurology 58, 1327-1332.
Wang, J., Wang, L., Zang, Y., Yang, H., Tang, H., Gong, Q., Chen, Z., Zhu, C., He, Y., 2009. Parcellation-dependent small-world brain functional networks: a resting-state fMRI study. Hum Brain Mapp 30, 1511-1523.
Wang, X.J., 2010. Neurophysiological and computational principles of cortical rhythms in cognition. Physiol Rev 90, 1195-1268.
Xia, M., Wang, J., He, Y., 2013. BrainNet Viewer: a network visualization tool for human brain connectomics. PLoS ONE 8, e68910.

Yuval-Greenberg, S., Tomer, O., Keren, A.S., Nelken, I., Deouell, L.Y., 2008. Transient induced gamma-band response in EEG as a manifestation of miniature saccades. Neuron 58, 429-441.

## Figure Legends

**Figure 1. Validation of the behavioral distinction between wakefulness and sleep data**. A) Low-pass filtered (dark lines) Dimension of Activation (DA) scores averaged across channels (light lines) were consistently above the cut-off score of 5 on wake condition and consistently below it on sleep condition. B) Histogram of the non-parametric permutation test t-values and t-value of the original comparison (dotted vertical line). No permuted comparison yielded a statistic above the obtained in the original comparison. C) Distribution of DA values for each condition.

**Figure 2. Connectivity analysis results for each subject, condition and frequency band.** A) Violin plot of wPLI distributions. Vertical dotted lines indicate extremes and median. Vertical axes correspond to frequency bands and horizontal axes to wPLI values. B) *Left*: channel-by-channel matrix representation of wPLI values. Vertical and horizontal axes represent electrodes, ordered and color-coded by lobe. Colormap indicates wPLI values. Within-subject top panels indicate wake condition and bottom panels indicate sleep condition. *Right:* Electrode location by subject, color-coded by lobe. wPLI: weighted Phase Lag Index.

**Figure 3. Connectivity vs. distance correlation matrix.** Pearson's correlation coefficient between connectivity values and Euclidean distance for each subject, condition and frequency band.

**Figure 4. Network-based analysis.** *Upper panels*. Normalized mean degree (lines) and standard deviation (shades) as a function of thresholding value. *Lower panels*. Welch *t*-value as a function of threshold. Shaded area represents $p < .05$ after correction for multiple comparisons. Color represents condition with higher mean. Within-subject panels correspond to frequency bands. wPLI: weighted Phase Lag Index. A) Results for the γ-range. B) Results for the remaining canonical frequency bands.

**Figure 5. Power analysis.** Violin plots of the power estimates for each subject and frequency band. Horizontal lines represent extremes and mean of the distributions. $p_n$: p-value based on the number of suprathreshold permutation tests, corrected for multiple comparisons using the Holm-Bonferroni method.

**Table 1. Generalized Estimating Equations analysis.** A) Estimates and significance tests of each predictor and their interactions for the model with high-γ connectivity. B) Ranking of goodness-of-fit of the

models for each frequency band (lower values indicate better fit). QIC: quasi-likelihood under the independence model criterion. *** $p < .001$

**Figure 6. Logistic curve of the high-γ predictor of the Generalized Estimating Equations model.** Histograms represent distribution of mean wPLI values for each condition. wPLI: weighted Phase Lag Index.

**Figure 7. Electrode location and mean high-γ wPLI for each subject.** Within-subject *top* and *bottom* panels correspond to wake and sleep conditions respectively. Color represents mean wPLI values and symbols denote subjects. wPLI: weighted Phase Lag Index.

**Figure 8. Combined electrode location and mean high-γ wPLI.** *Top* and *bottom* panels correspond to wake and sleep conditions respectively. Color represents mean wPLI values and symbols denote subjects. wPLI: weighted Phase Lag Index.

**Figure 9. High-γ wPLI by anatomical region for each subject.** Circles represent mean-wPLI value and lines represent Inter Quartile Range (IQR). Areas are shown in descending order of mean wPLI in the *wake* condition. Squares' colours represent corresponding brain lobes of anatomical regions. Asterisks denote statistical significance (corrected for multiple comparisons). Region names follow the Automated Anatomical Labeling naming-convention. Frontal Inf Tri: inferior frontal gyrus pars triangularis; Cingulum Ant: anterior cingulate gyrus; Frontal Inf Oper: inferior frontal gyrus pars opercularis; Supp Motor Area: supplementary motor area; Frontal Mid: middle frontal gyrus; Frontal Sup Medial: superior frontal gyrus medial part; Supra-marginal: supramarginal gyrus; Rolandic Oper: rolandic operculum; Temporal Mid: middle temporal gyrus; Frontal Sup: superior frontal gyrus; Temporal Sup: superior temporal gyrus; Temporal Pole Sup: superior temporal pole; Temporal Inf: inferior temporal gyrus; Fusiform: fusiform gyrus; Parietal Inf: inferior parietal lobule; Cingulum Mid: middle cingulate gyrus; Occipital Mid: middle occipital gyrus; Calcarine: calcarine sulcus; Occipital Sup: superior occipital gyrus; Parietal Sup: superior parietal lobule; Para-hippocampal: parahippocampal gyrus; Occipital Inf: inferior occipital gyrus; Angular: angular gyrus; Cingulum Post: posterior cingulate gyrus; wPLI: weighted Phase Lag Index; n.s.: non-significant (alpha-level: 0.05); * $p < .01$; ** $p < .001$